Desalination and Water Treatment
www.deswater.com

doi: 10.5004/dwt.2017.20252

65 (2017) 31–42
February

Measurement of transparent Alcian blue-stainable materials in freshwater by a centrifugation-based method

Nguyen Thi Thuy[a,b], Chihpin Huang[a,c], Justin Chun-Te Lin[c,d,*]

[a]*Institute of Environmental Engineering, National Chiao Tung University, Hsinchu 300, Taiwan*
[b]*Faculty of Biotechnology and Environmental Engineering, Ho Chi Minh City University of Food Industry, Vietnam, Tel. +84 903 250 375; email: thuyng3@gmail.com*
[c]*Disaster Prevention and Water Environmental Research Center, National Chiao Tung University, Hsinchu 300, Taiwan, Tel. +886-3-5712121 Ext. 55507; email: cphuang@mail.nctu.edu.tw*
[d]*Department of Environmental Engineering and Science, Feng Chia University, Taichung 407, Taiwan, Tel. +886-4-24517250 Ext. 5216; Fax: +886-4-24517686; email: jlin0623@gmail.com*

Received 2 May 2016; Accepted 4 October 2016

ABSTRACT

Transparent exopolymer particles (TEP) are particularly abundant in diverse aqueous environments and regarded as a main contributor to biofilm and membrane biofouling. In this study, we optimized a centrifugation-based approach to analyze Alcian blue-stainable materials (ABSM), which cover TEP and acidic polysaccharide-related substances, for reservoirs in Taiwan. Stability of the dye in terms of time and acidic conditioning was firstly monitored intensively at pH 2.5 and 4.0, with and without stirring. Absorbance of dye-reacted solutions of the reference materials (xanthan gum) and natural ABSM sampled from reservoirs were both examined under different relative centrifugal forces (RCF). Separation efficiency of complexes generated between Alcian blue and the targeting materials under broad range of RCFs (from 1,089 to 34,957 ×G) was further assessed based on particle hydrodynamic size distributions, which then provided an insight of their fates that former methods were not addressed. Our results showed centrifugation at high RCFs (higher than 12,096 ×G) was effective to separate these complexes comparing with previous studies only conducted at lower RCFs. Application of the proposed method for five freshwater samples revealed notable high concentrations of Alcian blue-stainable dissolved fraction that could be a critical factor in developing feasible antifouling strategies for membranes used in water treatment.

Keywords: Transparent exopolymer particles; Alcian blue; Membrane fouling agent; Centrifugation; Particle hydrodynamic size distributions; Acidic polysaccharide

1. Introduction

Transparent exopolymer particles (TEP) are regarded as a main contributor to biofilm and membrane biofouling [1–4]. These particles are particularly abundant in diverse aqueous environments and participate in a wide range of processes that are important in environmental science, such as microbial loop in aquatic food chains [5], aggregation web [6], biogeochemical processes [7], marine carbohydrate chemistry [8] and even the global carbon cycle [9]. However, TEP actually only represent a small fraction from the whole spectrum of the materials stainable with Alcian blue (AB) in aquatic environment. Colloid and dissolved fractions of these materials have been found in significant larger amounts compared with TEP [10–12].

Current methods for analyzing TEP suffer from containing highly sophisticated steps and from matrix effects (e.g., pH, ionic strength, and interactions with other dissolved organic matter) of various environmental samples. Previous methods of quantifying TEP can be categorized into three groups [2] that are: (1) microscopic numeration,

* Corresponding author.

(2) spectrophotometry and (3) centrifugation. While microscopic numeration and spectrophotometry are the most commonly used methods, centrifugation-based approach have appeared in a few studies only [13–15]. Microscopic counting methods are considered to be absolute analytical methods, which require no calibration, and units are typically per unit volume. In contrast, comparative analytical methods (of the second and third types) require calibration against known standards, e.g., xanthan gum (XG). The original TEP quantification method that was developed by Passow and Alldredge [16] has been well accepted, using AB staining on membranes with pore size of 0.4 μm at pH 2.5. Villacorte et al. [17] modified the method and extended to more membranes (0.4, 0.2, 0.1, and 0.05 μm), and introduced particle fraction of TEP (pTEP) for particular form (particles retaining on the 0.4 μm membrane) and colloid fraction of TEP (cTEP) for colloidal form (particles pass through 0.4-μm membrane, but retaining on 0.05-μm membrane). Difficulties in determining TEP via the current methods result from: (1) weighting of XG, which is very sensitive to inaccuracies even with a precise microbalance; (2) preparing uniform XG standard solution; and (3) the bulky dye (AB) used for staining either TEP or acidic polysaccharides (APS), which is also not easy to work with [18]. Moreover, versatile TEP protocols developed by various laboratories made the comparison of individual data rather difficult [2,18]. By taking into account the fact that smaller size fractions are even more abundant that TEP, the later methods were developed to determine not only TEP but also those fractions. Thornton et al. [10] proposed a method to quantity APS, which contain carboxyl, phosphate or sulfuric ester groups and are regarded as major components of TEP, in marine and freshwater [10]. In this method, the complexes of AB and APS were created in original water samples and then separated by filtration using different types of filters. The latest improved method was developed by Villacorte et al. [19] in which TEP and its precursors were firstly separated by another membrane with cutoffs at 10 kDa (TEP_{10kDa}), then resuspended in ultrapure water, and stained by AB. In final step, the complexes created from this method were also separated by filtration.

In contrast to labor-intensive and skillful procedure using membrane filters in the aforementioned methods, another approach applied centrifugation for the separation [13]. The staining reaction was firstly carried at pH 4 and centrifugation (3,000 rpm, 2,160 ×G, 30 min) was then introduced to separate the complexes created between AB and TEP. Later, this method was adopted in another study with some modifications, and centrifugation was conducted at 3,200 ×G [14]. Advantages of this method were simple and rapid as the separation process was conducted in the solution rather than on the membranes while better coefficients of variations were obtained. However, the size of TEP determined via such method was not clear. Possible error sources may result from applying tangential flow filtration cartridge (0.45 μm nominal pore size) to remove colloids and to concentrate the samples. Moreover, since a certain centrifugal force was directly applied for complex separation without giving any proof, these forces may not convince removal of AB–TEP precipitates completely. In another study, Ramus [15] used a higher force (i.e., 27,000 ×G) of centrifugation to analyze extracellular polymeric substances produced by soil alga that may need further investigation before being applicable for water environmental samples. Similarities and differences of each step in the historical TEP and APS determining methods, together with our proposed method, were compared as presented in Table 1.

Bar-Zeev et al. [3] reviewed TEP-related terminology and further elucidated TEP precursors ('nanogels' and 'dissolved fibrillary polymers') ranged in size from 5 to 400 nm, and TEP ('microgels' to 'macrogels') with a size of greater than 400 nm. Thuy et al. [12] proposed that 'Alcian blue-stainable materials' (ABSM) is a wider term for covering full range of these mentioned components. Although the underlying biofouling mechanisms of these material are not well understood, developing effective separation methods for the analytical process is essential for determining their physicochemical and biological properties. The aim of this study is to determine the effects of various relative centrifugal forces (RCF) on the separation of complexes created between AB and reference TEP (XG) or natural ABSM presenting in freshwater from reservoirs. To avoid confusion created by using the same terminologies (e.g., TEP or APS) though they were quantified by different methods [18], our target was referred as ABSM, as implied by the way the materials were determined. In addition, ABSM are not only confined to TEP but also confined to all particles and soluble materials stainable with AB in freshwater at pH 2.5. The method proposed here to quantify ABSM is rather complementary for the method proposed by Arruda Fatibello et al. [13], which determined particle TEP, by applying only a fixed RCF. In addition, we proposed using centrifugation as a simple alternative for the filtration used in Thornton et al. [10] to separate the complexes of AB and stainable compounds. In the first step, stability of AB staining dye solution was tested. UV–Vis spectrometry and dynamic light scattering (DLS) were then used to profile the absorbance and particle hydrodynamic size distribution (PSD) of the supernatants produced by various RCF. Finally, a centrifugation-based approach with optimum conditions was proposed and applied for freshwater sources, and the results yielded from this approach and former methods [11,16] were compared.

2. Materials and methods

2.1. Chemicals and apparatus

AB 8GX (analytical reagent grade), XG (from *Xanthomonas campestris*) and 37% formaldehyde solution were purchased from Sigma-Aldrich Co. LLC (USA). Two membrane filters, 0.4 and 0.05 μm polycarbonate (47 mm diameter), were obtained from Whatman Plc (UK). pH was measured using a benchtop pH meter (FiveEasy Plus, Mettler-Toledo, Switzerland) with a wide range electrode (pH 0–14, Temperature 0°C–100°C; InLab Expert Pro, Mettler-Toledo, Switzerland). A magnetic stirrer (Rexim RS 6DN, AS ONE Co., Osaka, Japan) was used for stirring AB solution. Two centrifuges used for separation were Table Top Centrifuge, Digisystem Laboratory Instruments Inc., Taiwan, and Avanti J-E, Beckman Coulter, Inc. The absorbance of the supernatants was measured at 610 nm using a UV–Vis spectrophotometer (SP 8001, Metertech Inc., Taiwan), and the particle hydrodynamic size was measured using a DLS particle analyzer (Nano ZS, Malvern Instruments Ltd., UK).

Table 1
Comparison steps in previous protocols for TEP, APS and method developed in this study

Steps	Protocol for TEP by Passow and Alldredge [16]	Protocol for TEP by Villacorte et al. [17]	Protocol for TEP by Arruda Fatibello et al. [13]	Protocol for APS by Thornton et al. [10]	Proposed method for Alcian blue-stainable material (ABSM)
Sample volume (mL); water types	1–500; seawater	40–200; estuarine, freshwater	80–100; freshwater	5; seawater, freshwater	30; freshwater
Sample pre-treatment (filtration)	0.4 μm PC[a] membrane	0.4, 0.2, 0.1 and 0.05 μm PC membranes	70 μm mesh nylon net and 0.45 μm cartridge in tangential filtration set	0.4 μm PC membranes; apply dialysis (1,000 Da) for seawater samples	0.4 and 0.05 μm PC membranes
Retained particles collection	Yes	Yes	No	No/yes[b]	No/yes[b]
Permeate collection	No	No	No	Yes	Yes
Staining phase	On the membranes	On the membranes	In 5 ml concentrated sample	In original sample and filtrates	In original sample and filtrates
Staining condition (Alcian blue solution)	0.5 mL of 0.02%, pH 2.5 (pre-filtered: 0.2 μm)	1 mL of 0.02%, pH 2.5 (pre-filtered: 0.05 μm)	0.5 mL of 0.06%, buffer pH 4	1 mL of 0.02%, pH 2.5 (pre-filtered: 0.2 μm)	5 mL of 0.02%, pH 2.5 (no pre-filtered)
Acidification	–	–	Buffer pH 4	pH 2.5	pH 2.5
Complexes separation	–	–	Centrifugation: 3,000 rpm (2,160 ×g); 30 min	Filtration by 0.1 and 0.2 μm PC membranes, 0.2 μm (SFCA[c]) and nylon syringe filters	Centrifugation: 0, 1,089, 3,024, 7,741, 12,096, 20,442, 27,216 and 34,957 ×g; 30 min
Absorbance measuring	Elute in 80% H_2SO_4, 787 nm	Elute in 80% H_2SO_4, 787 nm	In supernatant, 602 nm	In filtrate, 610 nm	In supernatant, 610 nm
Calibration by xanthan gum (XG)	Weighting of XG on filters by microbalance	Adopted from [16]	Weighting of XG by normal digital balance	Weighting of XG by normal digital balance	Weighting of XG by normal digital balance
Available results	TEP	pTEP and cTEP	TEP	APS in total and APS in filtrate	ABSM in raw water and filtrates

[a]PC – Polycarbonate.
[b]When TEP measurement enclosed, the step of retained particles collection is necessary.
[c]SFCA – Surfactant-free cellulose acetate.

2.2. Sample collection and storage

Freshwater samples were taken from four reservoirs of Taiwan: Pao-Shan Reservoir I, which provides drinking water for Hsinchu County; Tai-Hu and Tien-Pu Reservoirs, located in Kinmen County near south mainland China; and Sheng-Li reservoir in Lienchiang County. The dates for collecting samples were 3 and 27 January 2014 for two Pao-Shan samples; 15 August 2013 and 20 September 2014 for two Tai-Hu samples; 15 August 2013 for one Tien-Pu sample; and 25 August 2014 for one Sheng-Li sample. Each sample was collected in a 5-L bottle. The samples that were not immediately analyzed (within 6 h of sampling) were preserved in formalin (2 wt%) at 3°C until analysis.

2.3. Preliminary test of stability of dye solution

Since coagulation was observed in AB solutions over time, significantly reducing the AB concentration [16], the stability of the AB solution under centrifugation was monitored daily. Staining dye AB solutions were prepared at 0.06% (m/v) [13], in acetate buffer solution at pH 2.5 or 4. The AB solutions were either stored at 3°C (without stirring) or continuously mixed at 600 rpm (stirring) for 17 d.

Prior to centrifugation, the real concentration of these four AB standard solutions (pH 4.0 with/without stirring and pH 2.5 with/without stirring), denoted as (C_{AB}), were computed from the mass proportion of copper in each AB molecule ($C_{56}H_{68}C_{l4}CuN_{16}S_4$), as follows [17]:

$$C_{AB} = C_{Cu}/0.0489 \text{ (mg as AB L}^{-1}\text{)} \quad (1)$$

where the copper concentration (C_{Cu}) was determined from the absorbance of copper reagents (CuVer® 1, Cat. 2105869, Hach Co., USA) at a wavelength of 560 nm using a spectrophotometer (DR/4000U, Hach Co., USA).

To test the effect of centrifugation on the stability of these solutions, 0.5 mL AB solutions and 5 mL deionized (DI) water were added to 10 mL centrifuge tubes. These tubes were then filled up to 10 mL by adding 2.5 or 4 acetate buffer solutions. The contents in the centrifuge tubes were mixed for 1 min and centrifuged for 30 min at 1,066 ×G and 25°C. The absorbance of the supernatants was measured at a wavelength of 610 nm.

Because our proposed method tended to measure ABSM, covering both TEP and APS, AB solution was prepared following Passow and Alldredge [16], with a concentration of 0.02% (m/v) in acetate solution at pH 2.5, and stored at 3°C without stirring. Stability of this solution was investigated for over 50 d. Volume of 5 mL of the AB solution and 30 mL DI water were added to a 50-mL centrifuge tube, and the pH was also adjusted to 2.5. Mixing and centrifuging were carried out for the same periods as above, but at a higher centrifugal force of 12,096 ×G. Supernatants were also taken and measured absorbance.

2.4. Effects of centrifugal forces on absorbance and particle size distribution

Choice of RCF applied for complex separation will affect the particle size distribution (PSD) and absorbance of the supernatant. The ideal value is the one that can completely separate precipitates from the supernatant. To find the optimum speed, Tien-Pu sample were used to test the effect of various RCF on absorbance and PSD of the corresponding reacted solutions. The reaction solutions were made by adding 5 mL of AB solution (0.02% (w/v) AB, pH 2.5 without pre-filtration) to 30 mL water samples in a 50-mL centrifuge tube. The water samples here included four types: DI water, raw Tian-Pu sample, and its filtrates after 0.4 and 0.05 μm membrane filters. pH of these solutions was adjusted to 2.5 by the acetic acid. The centrifuge tubes were mixed for 1 min and centrifuged at eight RCFs: 0 (no centrifuge), 1,089 ×G (3,000 rpm), 3,024 ×G (5,000 rpm), 7,741 ×G (8,000 rpm), 12,096 ×G (10,000 rpm), 20,442 ×G (13,000 rpm), 27,216 ×G (15,000 rpm) and 34,957 ×G (18,000 rpm) for 30 min, at 25°C. Their supernatants were taken to measure absorbance (610 nm) and PSD. PSD was also measured for the supernatant of water samples (including raw sample and filtrates after 0.4 and 0.05 μm) under the same conditions (only without adding AB) for tracing and distinguishing between AB particle, water sample's particles, and complexes produced from above reaction solutions.

To test the effect of centrifuge speeds on absorbance of standard solutions, the XG solution was prepared by mixing 20 mg of XG into 200 mL DI water, ground with a 100-mL tissue grinder (Sunway Scientific Co., Taiwan), mixed for 30 min, and ground again to break apart the gel-like particles. The stock solution was diluted to five concentrations (1, 5, 10, 15 and 20 mg L^{-1}). 30 mL of each dilution was placed into centrifuge tubes and followed the same procedure above until absorbance measurement. Note that the three centrifuge speeds at 1,089, 12,096 and 27,216 ×G were applied in this experiment. Calibration curves were drawn based on the relationship between the XG concentration and the supernatant absorbance.

2.5. Demonstrations of proposed method in environmental matrix

Following previous experimental results, a method for analysis of various AB stainable fractions was proposed and demonstrated using Pao-Shan, Tai-Hu and Sheng-Li samples. Three fractions were introduced in this study based on the membranes used: (1) ABSM of raw water samples (denoted as $ABSM_{raw}$), (2) ABSM of filtrate from 0.4 μm membranes (denoted as $ABSM_{Fil\#1}$) and (3) ABSM of filtrate from 0.05 μm membranes (denoted as $ABSM_{Fil\#2}$), as illustrated in Fig. 1. In case of $ABSM_{raw}$ analysis, 30 mL raw sample was directly used without pre-treatment. For determining $ABSM_{Fil\#1}$ and $ABSM_{Fil\#2}$, 30–100 mL of the raw sample was successively filtered through 0.4 and 0.05 μm membranes, and 30-mL filtrates were collected subsequently into the centrifuge tubes. The remaining materials on the two membranes were, respectively, used to measure pTEP and cTEP (in section 2.6). 5 mL of the AB solution were added into the centrifuge tubes, and final pH was adjusted to 2.5 by acetic acid. The centrifuge tubes were mixed for 1 min, then centrifuged for 30 min at 12,096 ×G. The absorbance of the supernatant was measured at 610 nm [10].

Detection limit (DL) of our method was calculated according to Harvey [20]:

$$Abs_{DL} = Abs_{Bk} - z\sigma_{Bk} \quad (2)$$

where Abs_{Bk} is the mean absorbance of the blank, and σ_{Bk} is the standard deviation of ten independent measurements of the blank's absorbance, and z accounts for the desired confidence level.

2.6. TEP and other water quality parameters

This study also followed the methods proposed in Passow and Alldredge [16] and Villacorte et al. [17] to measure pTEP and cTEP concentrations in water samples. XG was used as a standard to calibrate TEP [16], and the calibration curve can be seen in Fig. S.1 in Supplementary material.

Other water quality parameters including temperature, pH, turbidity, total organic carbon (TOC), dissolved organic carbon (DOC), and chlorophyll *a* were measured immediately after sampling. To prepare DOC sample, raw water was filtered through the 0.4 μm polycarbonate filter.

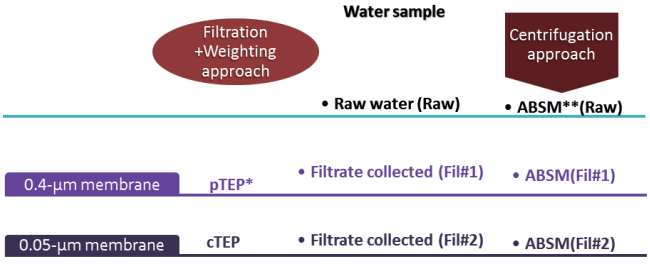

Fig. 1. Illustrations analytical protocols of pTEP, cTEP and Alcian blue-stainable materials determined in this study (*TEP: Transparent exopolymer particles, **ABSM: Alcian blue-stainable materials).

3. Results and discussion

3.1. Stability of AB under two acidic conditions and centrifugation

AB is used as a standard dye for staining the targeting substances (TEP and APS). Although this dye can selectively stain sulfated and carboxylated polysaccharides and various proteins (such as glycoproteins), it is regarded as 'not very easy to work with' [18]. The mechanism of interaction between the dye and the substrate is unknown, and various factors (such as pH, mixing conditions and reaction time) affect the stability of this dye. Though the effect of acidification ranged from pH 2.5 to 6.9 on analytical response was tested and the greatest linearity, highest sensitivity and lowest DL were found at pH 4 [13], most researchers use pH 2.5, as indicated in Table 1. In this study, the optimal acidification and storage condition of the dye were determined based on its stability under centrifugation.

As presented in Fig. 2, when AB solutions were simply kept at 3°C (i.e., without stirring), the absorbance of the AB solution's supernatant after centrifugation (1,066 ×G) was very stable at pH 2.5 (0.555 ± 0.002) while decreased from 0.521 (1st day) to 0.457 (17th day) with some fluctuations at pH 4. By taking into account that AB dye may settle by time, stirring was applied during storing of AB solutions. However, this stirring showed a worse effect on the stability of AB solutions, especially for the solution at pH 4 with its supernatant's absorbance decreased 25.1% from 0.530 (1st day) to 0.390 (17th day). At pH 2.5, the absorbance was approximately constant (0.613 ± 0.008) although the standard deviation was higher than that without stirring. Therefore, the application of stirring during storing was not recommended, and the AB solution prepared at pH 2.5 was preferred due to its better stability than that prepared at pH 4.

It is noted that prior to centrifugation, total AB concentration (including both dissolved and undissolved AB) of each AB solution was measured. Results yielded from this experiment showed that the real AB concentrations of four AB standard solutions (i.e., 0.055 ± 0.002, 0.056 ± 0.001, 0.058 ± 0.001 and 0.056 ± 0.001 wt% for the AB solutions prepared at pH 4.0 with/without stirring and pH 2.5 with/without stirring, respectively) were close to each other and to their original desired concentration (0.06 wt%). Hence, the absorbance decreases by time for pH 4. AB solutions under centrifugation, as mentioned above, suggest the existence of undissolved AB particles in the solutions, whose amount would increase by time due to settling and aggregation. In support of this finding, we observed some undissolved AB particles in AB solutions prepared at pH 4. In contrast, no particles were visible in the AB solution at pH 2.5.

Thus, AB solution was prepared at pH 2.5 and simply stored at 3°C in our proposed method. The stability of this solution under 12,096 ×G, which later was used in our protocol, was also confirmed by the insignificant variation of its supernatant's absorbance (0.574 ± 0.003) over 50 d (Fig. 2).

3.2. Effects of centrifugal forces on absorbance of standard solutions

Application of centrifugation for separation of complexes between AB and its stainable compounds was proposed by Arruda Fatibello et al. [13]. However, a RCF of 2,160 ×G (3,000 rpm) was directly applied without providing sufficient proof. In our research, centrifugation at three RCFs (1,089, 12,096 and 27,216 ×G) in 30 min was used to investigate the separation efficiency of complexes formed from the reaction between dye and XG (i.e., AB–XG complex particles). A wider XG concentration range (0–20 mg L^{-1}) than Arruda Fatibello et al.'s [13] work was tested. Results of calibration curves are displayed in Fig. 3, and details of their regression analysis is given in Table S.1 in Supplementary material. As can be seen, the slopes of the regression were negative because the absorbance decreased (color was removed) as the concentration of XG in the standard solutions increased. Excellent linear relationships (R^2 = 0.96 and 0.98) between XG concentration and absorbance at high RCF (12,096 and 27,216 ×G) were obtained over the full range of concentrations (0–20 mg L^{-1}). However, at a lower RCF (1,089 ×G), the linearity was reduced, with R^2 = 0.71 over the full range of concentrations and R^2 = 0.92 over

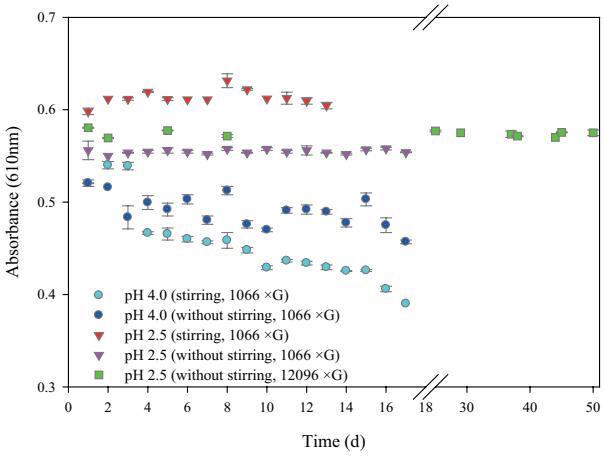

Fig. 2. Stability of Alcian blue solution with respect to pH (4.0 and 2.5), time (17 and 50 d) and centrifugal forces (1,066 and 12,096 ×G) (± standard deviation, n = 2).

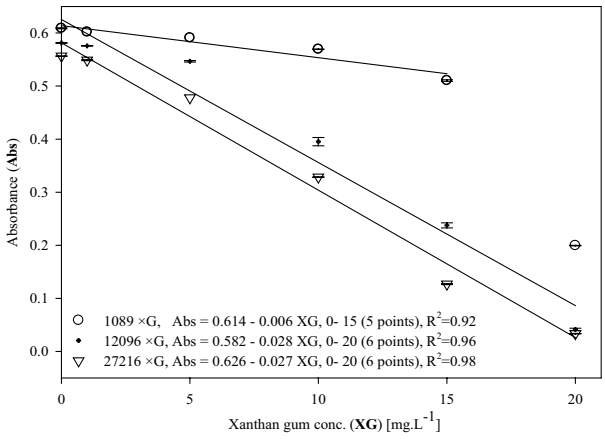

Fig. 3. Effects of centrifugal forces on absorbance of various xanthan gum concentrations. Each point shows the mean (± standard deviation, n = 4 for 12,096 ×G, n = 2 for 1,089 and 27,216 ×G).

a smaller range of concentrations (0–15 mg L^{-1}). Particularly, the absorbance was dropped by 67.2% from the initial point (no XG added) to the highest XG concentration of 20 mg L^{-1}.

The sudden drop of absorbance at XG concentration of 20 mg L^{-1} under 1,089 ×G can be further explained. Theoretically, XG was negatively charged and reacted with the hydrophilic cationic dye AB; the neutralization of surface charges of the particles causes destabilizing and eventually leads to the formation of aggregates as a result of coagulation process. The higher concentration of XG created the more amount of aggregates. These aggregates can entrain other aggregates, then create the bigger aggregates. Therefore, XG concentration at 20 mg L^{-1} would create flocs with bigger sizes compared with lower XG concentrations. The effect of particle size on sedimentation rate can be seen from Eq. (3) [21]:

$$v = \frac{d^2(\rho_p - \rho_m)}{18\mu} \times \mathrm{RCF} \quad (3)$$

where v is sedimentation rate; d is the diameter of the particle; ρ_p and ρ_m are the densities of medium and of the particle, respectively; and μ is the viscosity of the medium.

From Eq. (3), for particles with an identical density, the sedimentation of the larger particles will be faster, and the ratio of the velocities will follow a square law with respect to the ratio of the particle radii. Hence if we consider that the complexes in reaction solutions have the same density, larger one will be separated faster compared with smaller one under the same RCF. This explains that at a low RCF of 1,089 ×G, the centrifugation could remove mostly big size complexes, which were prevalently generated from staining reaction with high XG concentrations, particularly at 20 mg L^{-1}. Meanwhile, the smaller complexes that were mainly created from the staining reaction of lower XG concentrations could be partly separated from the solution. Hence, the unequal effects of this low RCF on different XG concentrations, due to the size of aggregates created, made the supernatant's absorbance drop sharply at some points corresponding to high XG concentrations (e.g., 20 mg L^{-1}), leading to the poor linearity between XG concentration and absorbance in the full range of XG concentration. In contrast, applying higher RCF (i.e., 12,096 and 27,216 ×G) could provide the forces strong enough to separate almost complexes in either small or big size available in the suspensions, resulted in the good linear coefficients between XG concentration and the induced absorbance.

For the low range of XG concentration (0–10 mg L^{-1}), our results at RCF of 1,089 ×G were consistent with the findings from Arruda Fatibello et al. [13], who used RCF of 2,160 ×G for the separation and achieved a good linear coefficient. We further suggested that expanding the XG concentration (up to 20 mg L^{-1}) required the centrifugation at higher RCF (i.e., 12,096 and 27,216 ×G) to get excellent linear coefficients of calibration curves. Compared with Thornton et al. [10], who used cellulose acetate membranes for the separation and achieved the linearity of calibration curves of 0.99 and 0.98 over XG concentrations of 0–15 and 0–5 mg L^{-1}, respectively, our study with centrifugation-based approach (at RCF of 12,096 and 27,216 ×G) gained comparable results. It is worth to note that our range of XG concentration was larger compared with Thornton et al. [10] and Arruda Fatibello et al. [13] that would offer the application for a wider range of concentration of ABSM available in various water samples.

3.3. Effects of centrifugal force on absorbance of real water samples

In this section, centrifugation at various RCF was carried out to investigate their separation efficiencies for the complexes between AB (dye) and its stainable materials in real water. RCF from 1,089 ×G (3,000 rpm) to 34,957 ×G (18,000 rpm) were applied uniformly for 30 min, and the changes in the absorbance and particle hydrodynamic size of the supernatants were measured. According to the origin of the water samples, their supernatants were indicated as Bk_{sup} for DI water (DI, as blank), Raw_{sup} for raw water sample from Tien-Pu Reservoir, $Fil\#1_{sup}$ for the 0.4 μm filtrate and $Fil\#2_{sup}$ for 0.05 μm filtrates, as schematically illustrated in Fig. 1. Some water quality parameters of Tien-Pu Reservoir can be seen in Table S.3.

The columns in Fig. 4 present raw data on the absorbance of the four supernatants. As can be seen, all of the four supernatants did not significantly differ in absorbance if no centrifugation was applied. When RCF was eventually increased to 34,957 ×G, the absorbance of Raw_{sup}, $Fil\#1_{sup}$ and $Fil\#2_{sup}$ decreased from very similar values (0.627, 0.627 and 0.663) to various amounts (0.222, 0.233 and 0.421, respectively). In contrast, absorbance of the blank's supernatant only slightly decreased from 0.664 to 0.556. The phenomena can be explained as no complex particles being created in the blank sample; therefore, centrifugation weakly affected its absorbance.

To elucidate the discrepancies in the absorbance among the supernatants from the blank and the three reaction solutions, three subtractions were introduced. The top of Fig. 4 illustrates the three subtractions at various RCF through presenting as a line-and-scatter plot referring to the right axis (ΔAbs). The subtractions of absorbance between the reaction solutions of DI and the 0.05 μm filtrate, marked as [$Abs(Bk_{sup})$ – $Abs(Fil\#2_{sup})$], were highly linear (R^2 = 0.998) at low RCF, and rose insignificantly (0.124 ± 0.008) when higher centrifugal speeds (12,096 and 34,957 ×G) were applied. The two

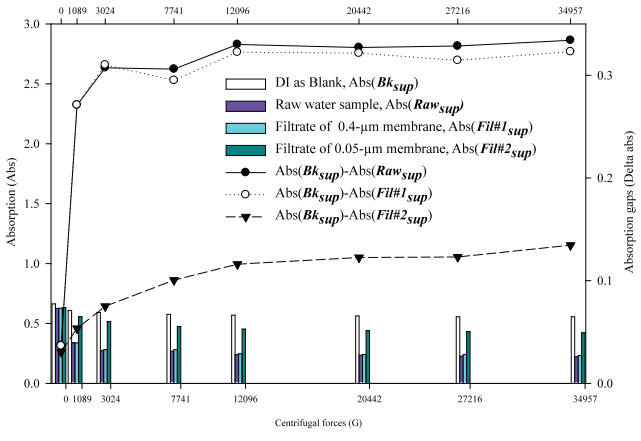

Fig. 4. Effects of centrifugal forces on absorbance (610 nm) of the supernatants.

other subtractions, denoted as [Abs(Bk_{sup}) – Abs(Raw_{sup})] and [Abs(Bk_{sup}) – Abs($Fil\#1_{sup}$)], obtained at RCF of less than 3,024 ×g were almost the same. Increasing RCF from 3,024 ×g then could promote the separation of large complexes between AB and its stainable compounds with a size of larger than 0.4 μm, which were available in raw water sample but not in Fil#1, leading to the appearance of a gap between two lines of these subtractions. At high RCF (from 12,096 to 34,957 ×G), both [Abs(Bk_{sup}) – Abs(Raw_{sup})] and [Abs(Bk_{sup}) – Abs($Fil\#1_{sup}$)] remained stable (0.322 ± 0.012 and 0.314 ± 0.011, respectively). Overall, the changes of three subtractions were insignificant at the RCF from 12,096 ×G.

3.4. Effects of centrifugal forces on hydrodynamic size of particles of real water samples

The efficiency of separation of complex particles was further analyzed by DLS. The same supernatants of the reaction solutions made from DI water (blank) (Bk_{sup}), sample Tien-Pu (Raw_{sup}), its 0.4 μm filtrate ($Fil\#1_{sup}$) and 0.05 μm filtrate ($Fil\#2_{sup}$) were used to study the effects of RCF on their PSD. DLS measurement could not be made for Raw_{sup} and $Fil\#1_{sup}$ because of the availability of some particle with the sizes higher than the upper limits for DLS (10,000 nm). Therefore, only PSD of particles in Bk_{sup} and $Fil\#2_{sup}$ were obtained, and plotted in Figs. 5(a) and (b), respectively.

Without centrifugation, the black line (Bk_{sup}) in Fig. 5(a) indicates that PSD of the pure dye particles consisted of the largest peak area (Pk1), from 60 to 500 nm, representing 93.9% of all particles while that of the second peak area (Pk2), from 28 to 60 nm, representing the remaining 6.1% of particles (Table S.2 in Supplementary material). Since the blank solution was made by dissolving AB powder in DI water, the particles in Bk_{sup} were undissolved AB particles or impurities (if have) in the solution. As displayed in the Fig. 5(b), the supernatant of reaction solution of 0.05 μm filtrate ($Fil\#2_{sup}$) showed PSD of 295–955 nm (Pk1) and 28–50 nm (Pk2) with very similar ratios of distribution peaks compared with that of Bk_{sup}: Pk1 area representing 93.5% of all particles, while Pk2 area counting the rest of 6.5%. Notably, although mean size of the particles in the minor peak from $Fil\#2_{sup}$ (Pk2, 41.6 nm) was very close to that in Pk2 of Bk_{sup} (40.1 nm), the mean size of the particles associated with Pk1 from $Fil\#2_{sup}$ (553.0 nm) was much larger than that associated with in Bk_{sup} (188.0 nm). This would evidence the generation of a complex compound between AB and its stainable compounds in $Fil\#2_{sub}$. Observation from Fig. 5 further reveals that as the centrifugal forces increased, the size of particles in two supernatants became smaller and more homogeneous, and eventually were almost integrated at high centrifugal forces (12,096, 27,216 and 34,957 ×G).

To determine the mechanism of centrifugation affecting the particle size and distribution percentage of particles, the raw data in Table S.2 are presented in a new figure. As displayed in the top of Fig. 6, increasing the centrifugal force did not significantly affect the mean size of the secondary peak (Pk2) of either Bk_{sup} or $Fil\#2_{sup}$. Over the full range of investigated centrifugal forces, the mean sizes of Pk2 from both Bk_{sup} and $Fil\#2_{sup}$ were stable with small standard deviations (32.2 ± 4.8 and 43.4 ± 12.3 nm, respectively). With respect to the major particles associated with the primary peak (Pk1), the mean size of those in Bk_{sup} fell from 188 to 91 nm as the centrifugal speed increased from 0 to 34,957 ×G. In contrast, the mean size of those in $Fil\#2_{sup}$ decreased in two steps, initially from 533 to 142.7 nm when centrifugal forces increased from 0 to 12,096 ×G, and then gradually from 142.7 to 109 nm when the forces further increased to 34,957 ×G. This phenomenon explains two effects: (1) the particles in the supernatant Bk_{sup} were weakly affected and removed by centrifugation because they comprised only the dye and (2) the two-stage decrease in the hydrodynamic sizes of particles in $Fil\#2_{sup}$ indicated centrifugation reached its limit in separating complex particles at 12,096 ×G (10,000 rpm). The complex particles at this centrifugal force can therefore be regarded as totally separated from the supernatant so the remaining particles in the solutions were mainly AB particles.

As plotted in the bottom of Fig. 6, the areas of the primary particles (Pk1) of Bk_{sup} and $Fil\#2_{sup}$ decreased from 93.9% and 93.5% to 71.0% and 58.1%, respectively, as the centrifugal forces increased from 0 to 34,957 ×G. Reversely, the areas of the secondary peaks (Pk2) of Bk_{sup} and $Fil\#2_{sup}$ increased from 6.1% and 6.5% to 29.0% and 34.9%, respectively. The shifts in these percentage areas were in support of the above

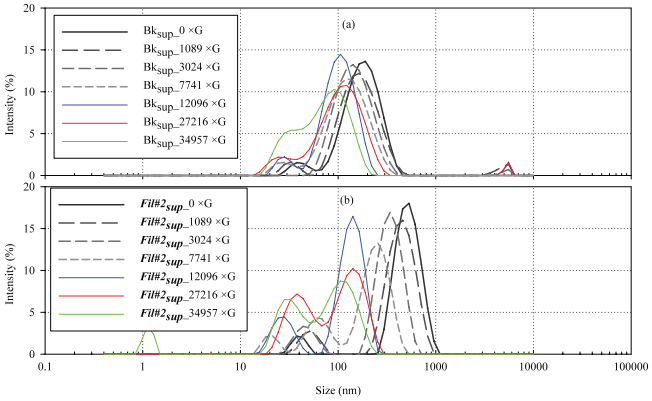

Fig. 5. Effects of relative centrifugal forces on particle hydrodynamic size distribution of (a) the blank's supernatant (Bk_{sup}) and (b) the reaction solution's supernatant ($Fil\#2_{sup}$).

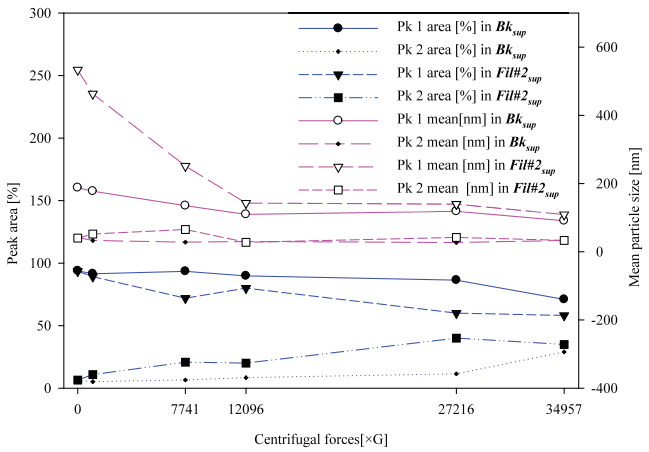

Fig. 6. Effects of relative centrifugal forces on the two major peaks (Pk1 and Pk2) of the blank's supernatant (Bk_{sup}) and the reacted solution's supernatant ($Fil\#2_{sup}$) in the DLS measurements.

observation that the particle sizes became more homogeneous at higher centrifugal forces.

Investigating PSD of particles in Bk_{sup} and $Fil\#2_{sup}$ can therefore help elucidate the effect of centrifugal forces on the separation of AB particles and complex particles from these supernatants. Regardless the experiment either for XG standard solutions (section 3.2) or for real water sample (Tien-Pu sample; section 3.3 and this section), the results consistently revealed that the high centrifugal forces (12,096 and 27,216 ×G) could separate mostly big and small complexes available in reaction solutions while smaller forces could only partly remove them.

3.5. Proposed method and its application in environmental matrix

The results obtained from previous sections were used to propose an analytical method for ABSM in freshwater samples. Since AB solutions change and aggregate by time [22,23], freshly preparing this solution was recommended in previous studies [17,24,25]. Our study revealed that AB solution prepared at pH 2.5 and kept at 3°C would maintain its stability, as assessed by the absorbance after centrifugation, for at least about 2 months. Based on the variations of the supernatant's absorbance and PSD under various RCF, RCF of 12,096 ×G was selected in our protocol, instead of lower RCF as suggested in previous studies [13,14], to reassure the complex separation. Calibration curve of this method was the second line in Fig. 3 (at RCF of 12,096 ×G), and the corresponding linear equation is the second one given in Table S.1. The large range of XG concentration (0–20 mg L^{-1}) used in making the calibration curve would offer the applicability of our method for various concentrations of ABSM in freshwater samples.

To determine the DL of the proposed method, $z = 3$ was selected, so 0.135% of measurements of the absorbance of the blank fall outside the specified range. The concentration of ABSM at the DL was determined from the absorbance at the DL and calculated from the slope (0.028) of the calibration curve at centrifugal force of 12,096 ×G, according to Eq. (4):

$$ABSM = [Abs_{Bk} - Abs_{DL}]/0.028 = z\sigma_{Bk}/0.028 = 0.461 \text{ mg } L^{-1} \quad (4)$$

Hence, DL of the proposed method was 0.461 mg L^{-1}, which was comparable with the DL yielded from Arruda Fatibello et al. [13] (i.e., 0.10 mg L^{-1}) and Villacorte et al. [19] (i.e., 0.91 mg L^{-1} for unconcentrated samples and 0.09 mg L^{-1} for concentrated samples).

Five environmental samples taken from three drinking water reservoirs were used to demonstrate the application of the proposed method. Different water quality parameters of these samples can be found in Table S.3 in the Supplementary material. TOC and DOC of these samples expressed a wide range from 0.9 to 14.3 mg L^{-1}. Similarly, chlorophyll *a* concentrations ranged from 2 to 36.7 μg L^{-1} while not much difference between these samples was found in pH (8.63 ± 0.40).

As presented in Fig. 7(a), pTEP from five water samples ranged widely from 0.0041 to 1.086 mg XG eq. L^{-1}. These concentrations were within the range of pTEP concentrations in freshwater sources found in the literature, as given in Table S.4 in the Supplementary material. The highest concentrations were found in Tai-Hu samples as we anticipated from their high concentrations of TOC, DOC and chlorophyll *a* compared with remaining samples (Table S.3). cTEP) was always significantly higher than the particle fraction, with a range of 0.247–7.305 mg XG eq. L^{-1}, dominating from 63% to 98% of total TEP. The highest cTEP in $Tai\text{-}Hu_1$ sample was also not in the range of reported values (Table S.4 in the Supplementary material).

Concentrations of different fractions of ABSM from five water samples were successfully measured by our centrifugation-based method, as presented in Fig. 7(a), with very low relative standard deviations of 0.2%–1.4% compared with previous methods [18]. ABSM in raw water samples were 7.297 ± 1.782 mg XG eq. L^{-1} with the highest values also found for Tai-Hu samples. Concentrations of $ABSM_{Fil\#1}$ and $ABSM_{Fil\#2}$ were from 70% to 98% of $ABSM_{raw}$, indicating that ABSM were mainly in the dissolved fractions. Though all these values were lower than acid polysaccharides concentrations (APS) previously reported in two freshwater ponds in Texas A&M University (11.87 ± 0.76 and 21.37 ± 0.05 mg XG eq. L^{-1}) [10], the notable high concentrations of ABSM in the filtrates of all samples were consistently found in both studies. This finding raises the importance of this small size fraction in future study, particularly in membrane technology as this fraction is more persistent against filtration process, even for low pore size membranes such as nanofiltration and reverse osmosis.

Since we conducted ABSM assay at the same pH, using the same AB dye solution and XG standard for calibration as TEP measurement, these two parameters can be directly compared. If we assume the subtraction between $ABSM_{raw}$

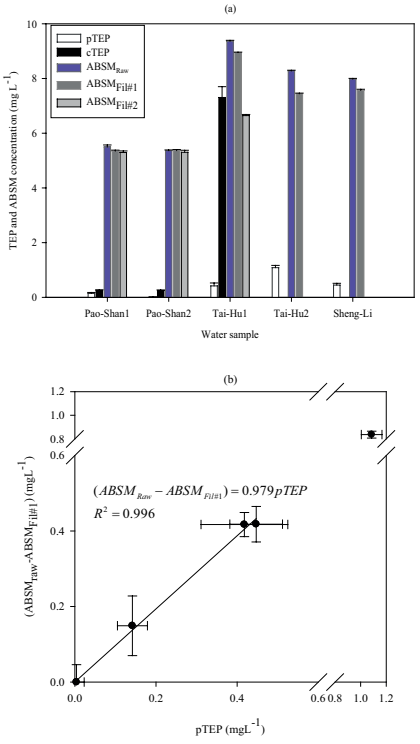

Fig. 7. (a) Demonstrations of ABSM and TEP fractions in five freshwater samples (average ± standard deviation, $n = 4$ or 5) and (b) comparison between pTEP and ($ABSM_{raw}$ – $ABSM_{Fil\#1}$) (error bars of pTEP and ($ABSM_{raw}$ – $ABSM_{Fil\#1}$) are standard deviation and propagated errors, respectively, $n = 4$).

and $ABSM_{Fil\#1}$ showing the amount of ABSM retained on 0.4 μm filter, hence the subtraction should be equivalent to pTEP. The main difference between the measurements of pTEP and ABSM is the staining reaction performed either on the filter (for pTEP) or in water samples themselves (for ABSM). Similarly, the subtraction of $ABSM_{Fil\#1}$ and $ABSM_{Fil\#2}$, and cTEP could be likely presenting the same amount of the stainable materials retained on 0.05 μm filter.

To test these hypotheses, a direct comparison was made between the results of TEP and ABSM as illustrated in Fig. 7(b). A strong linear relationship (R^2 = 0.99) was found between pTEP and ($ABSM_{raw}$ – $ABSM_{Fil\#1}$), suggesting the consistence between two parameters. It is noted that for Tai-Hu_2 sample, which contained a high amount of ABSM, the difference between pTEP and ($ABSM_{raw}$ – $ABSM_{Fil\#1}$) would be magnified, as the final point in Fig. 7(b). It is possibly due to the clogging of 0.4 μm membrane filter, though different sample volumes were tested for TEP analysis. Of course this clogging could happen in both pTEP and ABSM measurements for such type of sample, since they both used the membrane filtration process as a critical step and a pre-treatment step, respectively. However, only in case of pTEP measurement, where the staining reaction was performed on the membrane filter, this clogging could induce an excessive amount of AB retained on the filter, leading to the higher pTEP compared with ($ABSM_{raw}$ – $ABSM_{Fil\#1}$).

Similar comparison was performed for cTEP and ($ABSM_{Fil\#1}$ – $ABSM_{Fil\#2}$); however, only the result from Tai-Hu_2 sample can be used because the calculation of colloidal fractions of Pao-Shan samples by the subtraction of $ABSM_{Fil\#1}$ and $ABSM_{Fil\#2}$ resulted in high propagated errors. For Tai-Hu_2 sample, cTEP (7.305 ± 0.395 mg L^{-1}) was more than three times higher than the difference of $ABSM_{Fil\#1}$ and $ABSM_{Fil\#2}$ (2.305 ± 0.046 mg L^{-1}). Though we could not extend conclusion for colloid fractions due to the limited number of samples, we also anticipated a worse effect of clogging filter in cTEP measurement compared with pTEP, due to the smaller size of filter (0.05 μm) used in cTEP measurement. In addition, improperly using the calibration curve, which is originally designed for pTEP, to calculate cTEP would be another reason causing the uncertainty in cTEP measurement.

It is further noted that our method measured all compounds in water sources, which are stainable with AB, hence also included TEP and APS. Though AB is known as a specific stain for negatively charged polysaccharides [26], depending on the staining conditions, it may also bind through electrostatic interaction to other polyanions [27]. Thus, future studies focusing on what exactly the substances reacted with AB at specific conditions are still necessary to facilitate the comparison between the results yielded by different methods.

4. Conclusion

A centrifugal approach was optimized in order to measure ABSM, which covered TEP and APS. For the first time, we give an insight of the fates of the complexes resulting from the dye and the targeting ABSM under centrifugation. The proposed approach can be a simple alternative for filtration-based methods and complemented previous approaches also using centrifugation for TEP measurements, which were either carried out at single RCF only or lower RCFs without justification. The data yielded in this study for various freshwater samples could enrich the database of full spectra of ABSM and suggest the significance of small size fractions of ABSM in aquatic environments, which have been paid less attention compared with their particle fraction. Though it is not possible to be prescriptive about antifouling strategies, the results from this study suggest that ABSM could be used as a critical factor in developing these strategies.

Principal results obtained are summarized as follows:

- Stability of the dye was confirmed at pH 2.5 without stirring after a preliminary intensive monitoring for more than 2 weeks (17 and 50 d).
- Good correlations between XG concentrations and the reacted solutions' absorbance were achieved under three RCFs (1,089, 12,096 and 27,216 ×G). Investigating the effect of eight RCFs (from 0 to 34,957 ×G) on separation efficiency revealed that the complexes can be effectively separated by applying RCFs from 12,096 ×G.
- ABSM in five freshwater samples measured by the proposed method varied among sampling sites (average concentration of 7.297 ± 1.782 mg XG eq. L^{-1}). High amounts were found in both filtrates for all samples (70%–98% of those from raw samples), which indicated smaller size fraction is more abundant than the particle or colloidal fractions. The particle fraction analyzed through the proposed method was in agreement with pTEP, while colloid fraction was significantly lower than cTEP.

Acknowledgments

This work was supported by Ministry of Science and Technology, Taiwan under Grant (NSC 101-2221-E-033-031) and from National Chiao Tung University. Ted Knoy is appreciated for his editorial assistance.

References

[1] T. Berman, M. Holenberg, Don't fall foul of biofilm through high TEP levels, Filtr. Sep., 42 (2005) 30–32.
[2] S. Meng, M. Rzechowicz, H. Winters, A. Fane, Y. Liu, Transparent exopolymer particles (TEP) and their potential effect on membrane biofouling, Appl. Microbiol. Biotechnol., 97 (2013) 5705–5710.
[3] E. Bar-Zeev, U. Passow, S.R. Castrillon, M. Elimelech, Transparent exopolymer particles: from aquatic environments and engineered systems to membrane biofouling, Environ. Sci. Technol., 49 (2015) 691–707.
[4] T. Jamieson, A.V. Ellis, D.A. Khodakov, S. Balzano, D.A. Hemraj, S.C. Leterme, Bacterial production of transparent exopolymer particles during static and laboratory-based cross-flow experiments, Environ. Sci. Water Res. Technol., 2 (2016) 376–382.
[5] U. Passow, Transparent exopolymer particles (TEP) in aquatic environments, Prog. Oceanogr., 55 (2002) 287–333.
[6] A. Engel, S. Thoms, U. Riebesell, E. Rochelle-Newall, I. Zondervan, Polysaccharide aggregation as a potential sink of marine dissolved organic carbon, Nature, 428 (2004) 929–932.
[7] X. Mari, M. Robert, Metal induced variations of TEP sticking properties in the southwestern lagoon of New Caledonia, Mar. Chem., 110 (2008) 98–108.
[8] P. Verdugo, A.L. Alldredge, F. Azam, D.L. Kirchman, U. Passow, P.H. Santschi, The oceanic gel phase: a bridge in the DOM–POM continuum, Mar. Chem., 92 (2004) 67–85.
[9] K.R. Arrigo, Carbon cycle: marine manipulations, Nature, 450 (2007) 491–492.

[10] D.C.O. Thornton, E.M. Fejes, S.F. DiMarco, K.M. Clancy, Measurement of acid polysaccharides in marine and freshwater samples using alcian blue, Limnol. Oceanogr. Methods, 5 (2007) 73–87.
[11] L.O. Villacorte, R. Schurer, M.D. Kennedy, G.L. Amy, J.C. Schippers, The fate of transparent exopolymer particles (TEP) in seawater UF-RO system: a pilot plant study in Zeeland, The Netherlands, Desal. Wat. Treat., 13 (2010) 109–119.
[12] N.T. Thuy, J.C.-T. Lin, Y. Juang, C. Huang, Temporal variation and interaction of full size spectrum Alcian blue stainable materials and water quality parameters in a reservoir, Chemosphere, 131 (2015) 139–148.
[13] S.H.S. Arruda Fatibello, A.A. Henriques Vieira, O. Fatibello-Filho, A rapid spectrophotometric method for the determination of transparent exopolymer particles (TEP) in freshwater, Talanta, 62 (2004) 81–85.
[14] C. Pascal, P. Ian, L. Sebastien, V. Benoit, Effects of temperature on photosynthetic parameters and TEP production in eight species of marine microalgae, Aquat. Microb. Ecol., 51 (2008) 1–11.
[15] J. Ramus, Alcian blue: a quantitative aqueous assay for algal acid and sulfated polysaccharides, J. Phychol., 13 (1977) 345–348.
[16] U. Passow, A.L. Alldredge, A dye-binding assay for the spectrophotometric measurement of transparent exopolymer particles (TEP), Limnol. Oceanogr., 40 (1995) 1326–1335.
[17] L.O. Villacorte, M.D. Kennedy, G.L. Amy, J.C. Schippers, The fate of Transparent Exopolymer Particles (TEP) in integrated membrane systems: removal through pre-treatment processes and deposition on reverse osmosis membranes, Water Res., 43 (2009) 5039–5052.
[18] V. Discart, M.R. Bilad, I.F.J. Vankelecom, Critical evaluation of the determination methods for transparent exopolymer particles, agents of membrane fouling, Crit. Rev. Environ. Sci. Technol., 45 (2015) 167–192.
[19] L.O. Villacorte, Y. Ekowati, H.N. Calix-Ponce, J.C. Schippers, G.L. Amy, M.D. Kennedy, Improved method for measuring transparent exopolymer particles (TEP) and their precursors in fresh and saline water, Water Res., 70 (2015) 300–312.
[20] D. Harvey, Modern Analytical Chemistry, McGraw-Hill, New York, 1999.
[21] M.J. Waites, N.L. Morgan, J.S. Rockey, G. Higton, Industrial Microbiology: An Introduction, Blackwell Science, Oxford, 2001.
[22] R.W. Horobin, Dextrin and salt as impurities of histological dyes, Histochemie, 22 (1970) 39–44.
[23] D.J. Goldstein, R.W. Horobin, Rate factors in staining by Alcian Blue, Histochem. J., 6 (1974) 157–174.
[24] R. Jones, L. Reid, The effect of pH on Alcian Blue staining of epithelial acid glycoproteins. I. Sialomucins and sulphomucins (singly or in simple combinations), Histochem. J., 5 (1973) 9–18.
[25] K. Masuda, H. Shirota, E.J.M.A. Thonar, Quantification of 35S-labeled proteoglycans complexed to Alcian Blue by rapid filtration in multiwell plates, Anal. Biochem., 217 (1994) 167–175.
[26] U. Passow, A.L. Alldredge, Distribution, size and bacterial colonization of transparent exopolymer particles (TEP) in the ocean, Mar. Ecol. Prog. Ser., 113 (1994) 185–198.
[27] A. Hayat, Stains and Cytochemical Methods, Springer, USA, 1993.

Supplementary material

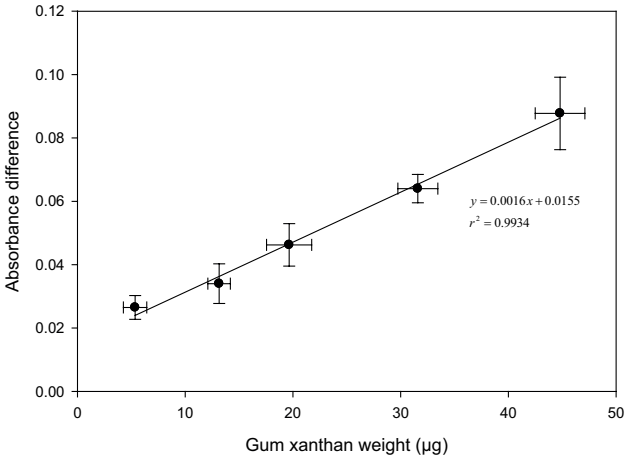

Fig. S.1. TEP calibration curve, weighting measurements for xanthan gum and absorbance for reactants were carried out four times (n = 4).

Table S.1
Calibration curves of xanthan gum (GX) concentrations in three different centrifugal forces

Centrifugal force (×G)	Equation	Linearity range (mg L^{-1})	R^2
1,089	Abs = 0.614 – 0.006 GX	0–15 (5 points)	0.92
12,096	Abs = 0.582 – 0.028 GX	0–20 (6 points)	0.96
27,216	Abs = 0.626 – 0.027 GX	0–20 (6 points)	0.98

Table S.2
Hydrodynamic size distribution results of the blank supernatant (Bk_{sub}) and the reacted solution's supernatant ($Fil\#2_{sub}$)

Sample description (×G)	PdI	Pk1 mean (nm)	Pk2 mean (nm)	Pk1 area (%)	Pk2 area (%)
Bk_{sup}, 0	0.387	188.0	41.6	93.9	6.1
$Fil\#2_{sup}$, 0	0.457	533.0	40.1	93.5	6.5
BK_{sup}, 1,089	0.282	177.7	32.9	91.5	5.2
$Fil\#2_{sup}$, 1,089	0.711	462.9	51.9	89.1	10.9
Bk_{sup}, 7,741	0.247	135.0	28.1	93.4	6.6
$Fil\#2_{sup}$, 7,741	0.428	251.2	65.2	71.9	20.8
Bk_{sup}, 12,096	0.356	109.7	30.0	89.8	8.4
$Fil\#2_{sup}$, 12,096	0.268	142.7	27.7	80.0	20.0
Bk_{sup}, 27,216	0.409	118.6	27.2	86.4	11.5
$Fil\#2_{sup}$, 27,216	0.215	139.4	41.9	60.0	40.0
Bk_{sup}, 34,957	0.193	91.0	33.1	71.0	29.0
$Fil\#2_{sup}$, 34,957	0.236	109.0	33.4	58.1	34.9

Note: PdI – Polydispersity index; Pk1 – peak of primary particle; Pk2 – peak of secondary particle; and only two main peaks with area >5% were considered.

Table S.3
Water quality parameters from six water samples

Sample name	Sampling date (year month date)	TOC (mg L^{-1})	DOC (mg L^{-1})	Temperature (°C)	pH	Turbidity (NTU)	Chlorophyll *a* (µg L^{-1})
$Pao\text{-}Shan_1$	2014 01 03	1.0	0.9	18.1	8.36	6.7	4.1
$Pao\text{-}Shan_2$	2014 01 27	1.3	1.2	14.8	8.26	2.7	2.1
$Tai\text{-}Hu_1$	2013 08 15	14.3	10.0	28.0	8.91	14.1	22.8
$Tai\text{-}Hu_2$	2014 09 20	11.9	8.9	–	–	10.2	36.7
Sheng-Li	2014 08 25	4.4	4.2	30.6	8.44	2.8	3.5
Tien-Pu	2013 08 15	17.4	13.3	28.0	9.20	24.7	34.6

Table S.4
pTEP and cTEP concentrations from various freshwater sources

Source	pTEP (mg XG eq. L^{-1})	cTEP (mg XG eq. L^{-1})	cTEP/total (%)	Reference
Canal	0.990 ± 0.127	–	–	[1]
Canal	~0.280	~1.640	85	[2]
Reservoir	~0.240	~0.430	65	[2]
River	0.060	0.210	78	[3]
Lake	0.110	0.500	82	[3]
Canal	0.070	0.360	84	[3]
Lake (Israel)	0.064–2.755	–	–	[4]
Lakes (southern Spain and north of USA)	0.036–9.038	–	–	[5]
Lake (Israel)	0.759–2.385	–	–	[6]
Surface water	0.015 ± 0.014	0.684 ± 0.094	98	[7]
Sallow lake	~0.050	~1.100[a]	–	[8]
Pao-Shan reservoir	0.088–0.604	0.258–2.153	–	[9]

[a]TEP10 kDa = TEP + precursor.

References

[1] M.D. Kennedy, F.P.M. Tobar, G. Amy, J.C. Schippers, Transparent exopolymer particle (TEP) fouling of ultrafiltration membrane systems, Desal. Wat. Treat., 6 (2009) 169–176.
[2] L.O. Villacorte, M.D. Kennedy, G.L. Amy, J.C. Schippers, Measuring transparent exopolymer particles (TEP) as indicator of the (bio)fouling potential of RO feed water, Desal. Wat. Treat., 5 (2009) 207–212.
[3] L.O. Villacorte, M.D. Kennedy, G.L. Amy, J.C. Schippers, The fate of Transparent Exopolymer Particles (TEP) in integrated membrane systems: removal through pre-treatment processes and deposition on reverse osmosis membranes, Water Res., 43 (2009) 5039–5052.
[4] T. Berman, R. Mizrahi, C.G. Dosoretz, Transparent exopolymer particles (TEP): a critical factor in aquatic biofilm initiation and fouling on filtration membranes, Desalination, 276 (2011) 184–190.
[5] I. de Vicente, E. Ortega-Retuerta, I.P. Mazuecos, M.L. Pace, J.J. Cole, I. Reche, Variation in transparent exopolymer particles in relation to biological and chemical factors in two contrasting lake districts, Aquat. Sci., 72 (2010) 443–453.
[6] T. Berman, R. Parparova, Visualization of transparent exopolymer particles (TEP) in various source waters, Desal. Wat. Treat., 21 (2010) 382–389.
[7] S. Van Nevel, T. Hennebel, K. De Beuf, G. Du Laing, W. Verstraete, N. Boon, Transparent exopolymer particle removal in different drinking water production centers, Water Res., 46 (2012) 3603–3611.
[8] L.O. Villacorte, Y. Ekowati, H.N. Calix-Ponce, J.C. Schippers, G.L. Amy, M.D. Kennedy, Improved method for measuring transparent exopolymer particles (TEP) and their precursors in fresh and saline water, Water Res., 70 (2015) 300–312.
[9] N.T. Thuy, J.C.-T. Lin, Y. Juang, C. Huang, Temporal variation and interaction of full size spectrum Alcian blue stainable materials and water quality parameters in a reservoir, Chemosphere, 131 (2015) 139–148.